Double Space-Time Transmit Diversity with Subgroup Rate Control for UMTS: Throughput Analysis

Christian Mehlführer, Markus Rupp
Institute of Communications and Radio-Frequency Engineering
Vienna University of Technology
Gusshausstrasse 25/389, A-1040 Vienna, Austria
Email: {chmehl, mrupp}@nt.tuwien.ac.at
Web: http://www.nt.tuwien.ac.at/rapid_prototyping

Christoph F. Mecklenbräuker
ftw. Forschungszentrum Telekommunikation Wien
Donau-City-Strasse 1, A-1220 Wien, Austria
Email: cfm@ftw.at
Web: http://www.ftw.at

***Abstract*— This paper deals with a detailed throughput analysis of the DSTTD-SGRC (Double Space-Time Transmit Diversity with Sub-Group Rate Control) proposal which is under consideration for the MIMO extension of UMTS. We examine different receiver structures for DSTTD-SGRC and compare them to the HSDPA SISO (Single-Input Single-Output) and the HSDPA STTD (Space-Time Transmit Diversity) transmission scheme, which was already standardized in the 3GPP. Furthermore, a Linear Minimum Mean Squared Error (LMMSE) receiver avoiding the usual matrix inversion, is derived. The output of our simulations are throughput curves that take, beside to the MIMO receiver, the coding and also the Hybrid Automatic Retransmission Request (HARQ) into consideration.**

I. Introduction

Release '99 of the UMTS standard specifies the so-called STTD mode [1] which is mandatory for the UE (User Equipment) and optional for UTRAN (Universal Terrestrial Radio Access Network). This STTD mode performs Alamouti coding [2] on the symbol stream to be transmitted and, thus, is able to achieve a transmit diversity order of two. A further increase in network throughput and spectral efficiency can be achieved by using even more antennas at the transmitter and receiver side [3], [4]. However, care must be taken on the design of the space-time code being employed, because the additional antennas can be either used for spatial multiplexing, increasing diversity order, or a tradeoff of both. Since it is not obvious which variant will have the best performance in terms of throughput, a detailed throughput analysis which takes channel coding and retransmissions into account, is necessary.

In the 3GPP technical report 25.876 [5] eight different corporate proposals for space-time coding are documented. This paper investigates the MERL (Mitsubishi Electric Research Laboratories) proposal, the so-called Double Space-Time Transmit Diversity with Sub-Group Rate Control (DSTTD-SGRC). The DSTTD proposal doubles the transmitter hardware needed for STTD and uses four instead of two transmit antennas. Therefore, the DSTTD scheme should be able to achieve twice the data rate and more than twice the spectral efficiency of the SISO transmission, at least in theory. Another advantage of DSTTD is its backward compatibility to the STTD mode. Thus, it also allows to serve users not capable of receiving DSTTD coded data to receive STTD data streams.

All simulations in this contribution are based on a UMTS Release 5 HSDPA simulator which is intended for analyzing various receivers on complying with the performance requirements specified in [6]. Since the performance requirements are always given at certain HS-PDSCH E_c/I_{or} (chip energy of the data stream over total radiated energy) values, our simulations were also performed over HS-PDSCH E_c/I_{or}.

The HSDPA simulator was developed at the ftw. throughout the projects C3 and C9. In this paper we only treat the extensions necessary for DSTTD transmission. A detailed description of the HSDPA simulator itself can be found in [7].

In Section II we explain the implemented DSTTD transmitter in more detail. Section III treats the channel and noise estimation used in the different implemented receiver structures. These DSTTD receivers are explained in detail in Section IV where we also derive an LMMSE receiver not requiring a matrix inversion. Furthermore, we introduce the MMSE-pSIC (MMSE with partial Successive Interference Cancelation) receiver which performs interference cancelation with hard decisions of the symbols obtained at the output of the LMMSE receiver. Section V deals with the throughput simulations and compares the various receiver structures and the different schemes (DSTTD, STTD, and SISO). Finally, we report our conclusions.

II. Implemented DSTTD Transmitter

This section describes the DSTTD scheme and its implementation. In the transmitter the data stream is first splitted by a serial to parallel converter into two subgroups. These subgroups are individually interleaved, coded, and punctured as specified in the HSDPA standard in 3GPP Release 5 [8]. After symbol mapping an Alamouti space-time coder is applied to each subgroup. In our simulations we considered one and two subgroups which correspond to two and four transmit antennas, respectively. Note, that the two antenna case

is equivalent to the STTD scheme because of the backward compatibility of DSTTD.

After space-time coding, the symbol streams are multiplexed onto several physical channels distinguished by different spreading (channelization) sequences. The actual number of spreading sequences assigned to one user is defined by the Node B depending on the data rate requirements and the channel quality of all users connected to the Node B. We will consider a fixed number of channelization codes throughout the paper to simplify the comparison between the differing schemes.

After spreading of the HS-PDSCH (High Speed Packet Downlink Shared Channel), a pilot channel (CPICH, Common Pilot Channel, SF=256) is added to the chip stream at each transmit antenna. Note, that pilot channels for more than two transmit antennas are not specified by 3GPP up to now. We used pilot channels which are orthogonal in groups of four symbols, as described in [9]. After adding the pilots to the data chip stream, scrambling is performed with the same scrambling sequence on all antennas. Then the synchronization channel is added at the first transmit antenna. Since the synchronization channel is transmitted unspread it causes interference on the data channels and has, therefore, impact on the system throughput. Reference [7] and [10] showed this impact of the synchronization channel on the throughput of SISO HSDPA and proposed a cancelation method that can be easily extended to MIMO HSDPA.

III. Channel and Noise Estimation

A. Channel Estimation

In our simulations we considered a flat block fading MIMO channel. Therefore, the MIMO channel can be represented as an $N_R \times N_T$ matrix, where N_R denotes the number of receive antennas and N_T the number of transmit antennas ($N_T = 4$ for DSTTD, $N_T = 2$ for STTD). The channel matrix was estimated by using the received pilot symbols of one subframe (30 pilot symbols per subframe and transmit antenna) in a least squares estimator. Since the pilot is normally transmitted with much less power than the HS-PDSCH, this estimation only yields the channel coefficients up to an unknown gain factor between the pilot and the data symbols. This gain factor is only known at the transmitter side and not signalled to the receiver. Therefore, the power of the received data symbols was calculated and divided by the estimated channel gain, which reveals the unknown gain factor of the HS-PDSCH. Note, that this channel gain estimation based on symbols also compensates for the different spreading factors of the HS-PDSCH and the CPICH.

B. Noise Variance Estimation

The various MIMO receivers implemented need an estimation of the noise variance on the HS-PDSCH. Additionally, the QPSK and 16-QAM soft demappers need estimates of the noise variance after the MIMO receivers to calculate log-likelihood ratios for the Turbo decoder. Whereas the latter can be calculated easily via the noise enhancement of the MIMO receiver, the noise variance on the HS-PDSCH was calculated by estimating the noise on the CPICH and correcting the variance with the before mentioned gain factor of the HS-PDSCH.

IV. Implemented Receiver Structures

A. Signal Model

For the derivation of the various receiver structures it is necessary to have a closer look at the underlying signal model. In this section we will only consider receivers for DSTTD since the STTD and SISO receivers become trivial in the case of flat fading transmissions. The received space-time coded signal can be written as

$$\mathbf{Y} = \left[\begin{array}{cc} \mathbf{y}_0 & \mathbf{y}_1 \end{array} \right] = \mathbf{HS} + \mathbf{V}, \tag{1}$$

where $\mathbf{y}_0$ denotes the received signal vector of dimension $N_R \times 1$ at time instant 0, $\mathbf{y}_1$ the received signal vector at time instant 1, $\mathbf{S}$ the space-time coding matrix, $\mathbf{V}$ the received noise, and

$$\mathbf{H} = \left[\begin{array}{cccc} \mathbf{h}_1 & \mathbf{h}_2 & \mathbf{h}_3 & \mathbf{h}_4 \end{array} \right] \tag{2}$$

the $N_R \times N_T$ channel matrix. The $\mathbf{h}_k$ are vectors of dimension $N_R \times 1$ containing the channel coefficients from transmit antenna k to all receive antennas. The space-time coding matrix $\mathbf{S}$ for DSTTD transmission is given by

$$\mathbf{S} = \left[\begin{array}{c} \mathbf{S}_a \\ \mathbf{S}_b \end{array} \right] = \left[\begin{array}{cc} s_1 & s_2 \\ -s_2^* & s_1^* \\ s_3 & s_4 \\ -s_4^* & s_3^* \end{array} \right], \tag{3}$$

where s_1 and s_2 denote the transmit symbols of subgroup 1 and s_3, s_4 the transmit symbols of subgroup 2. Note, that the matrices $\mathbf{S}_a$ and $\mathbf{S}_b$ are equivalent to the Alamouti space-time coding matrix.

By stacking two consecutive receive vectors $\mathbf{y}$ into one vector, (1), (2), and (3) can be reformulated to

$$\begin{aligned} \mathbf{r} &= \left[\begin{array}{c} \mathbf{y}_0 \\ \mathbf{y}_1^* \end{array} \right] = \mathbf{G}\mathbf{z} + \tilde{\mathbf{v}} = \left[\begin{array}{cc} \mathbf{H}_a & \mathbf{H}_b \end{array} \right] \mathbf{z} + \tilde{\mathbf{v}} = \\ &= \underbrace{\left[\begin{array}{cccc} \mathbf{h}_1 & -\mathbf{h}_2 & \mathbf{h}_3 & -\mathbf{h}_4 \\ \mathbf{h}_2^* & \mathbf{h}_1^* & \mathbf{h}_4^* & \mathbf{h}_3^* \end{array} \right]}_{\mathbf{G}} \underbrace{\left[\begin{array}{c} s_1 \\ s_2^* \\ s_3 \\ s_4^* \end{array} \right]}_{\mathbf{z}} + \tilde{\mathbf{v}}. \end{aligned} \tag{4}$$

The matrix $\mathbf{G}$ and the vectors $\mathbf{z}$ and $\tilde{\mathbf{v}}$ are modified versions of the channel matrix $\mathbf{H}$, the transmit symbols s_k and the noise matrix $\mathbf{V}$, respectively. The matrix $\mathbf{G}$ is a block matrix consisting of the two submatrices $\mathbf{H}_a$ and $\mathbf{H}_b$.

In the next subsections we consider various receiver structures, that calculate the transmitted symbols s_k from the received signal vector $\mathbf{r}$.

B. ZF/LMMSE Receiver

The ZF (Zero Forcing) and LMMSE (Linear Minimum Mean Squared Error) receivers are given by the pseudoinverse of $\mathbf{G}$. Thus, an estimate for the symbol vector $\mathbf{z}$ can be calculated by

$$\hat{\mathbf{z}} = \left(\mathbf{G}^H \mathbf{G} + \frac{\sigma_v^2}{\sigma_s^2} \mathbf{I}_{N_T} \right)^{-1} \mathbf{G}^H \mathbf{r}, \tag{5}$$

with the noise variance σ_v^2 (which is set to zero in case of the zero forcing receiver), the energy σ_s^2 of the zero mean symbols, and $\mathbf{I}_{N_T}$ the identity matrix of dimension N_T. Since the calculation of the pseudoinverse is very costly in hardware, it is desirable to find a simplified implementation avoiding the matrix inversion. Fortunately, this is possible due to the special structure of $\left(\mathbf{G}^H \mathbf{G} + \frac{\sigma_v^2}{\sigma_s^2} \mathbf{I}_{N_T} \right)$. The matrix $\mathbf{G}^H \mathbf{G}$ can be written as

$$\mathbf{G}^H \mathbf{G} = \begin{bmatrix} \mathbf{H}_a^H \mathbf{H}_a & \mathbf{H}_a^H \mathbf{H}_b \\ \mathbf{H}_b^H \mathbf{H}_a & \mathbf{H}_b^H \mathbf{H}_b \end{bmatrix}, \tag{6}$$

and by inserting the Alamouti matrices $\mathbf{H}_a$ and $\mathbf{H}_b$ we obtain

$$\left(\mathbf{G}^{\mathbf{H}} \mathbf{G} + \frac{\sigma_v^2}{\sigma_s^2} \mathbf{I}_{N_T} \right)^{-1} = \begin{bmatrix} h_a^2 \cdot \mathbf{I}_2 & \mathbf{H}_a^H \mathbf{H}_b \\ \mathbf{H}_b^H \mathbf{H}_a & h_b^2 \cdot \mathbf{I}_2 \end{bmatrix}^{-1}, \tag{7}$$

with

$$\begin{aligned} h_a^2 = &\quad \mathbf{h}_1^H \mathbf{h}_1 + \mathbf{h}_2^H \mathbf{h}_2 + \tfrac{\sigma_v^2}{\sigma_s^2} \\ h_b^2 = &\quad \mathbf{h}_3^H \mathbf{h}_3 + \mathbf{h}_4^H \mathbf{h}_4 + \tfrac{\sigma_v^2}{\sigma_s^2}. \end{aligned} \tag{8}$$

By inverting (7) analytically, it can be shown that the LMMSE receiver can be represented as

$$\begin{aligned} \left(\mathbf{G}^{\mathbf{H}} \mathbf{G} + \tfrac{\sigma_v^2}{\sigma_s^2} \mathbf{I}_{N_T} \right)^{-1} \mathbf{G}^H = \\ = \frac{1}{c} \cdot \begin{bmatrix} \mathbf{H}_a^H \left(h_b^2 \cdot \mathbf{I}_{2N_R} - \mathbf{H}_b \mathbf{H}_b^H \right) \\ \mathbf{H}_b^H \left(h_a^2 \cdot \mathbf{I}_{2N_R} - \mathbf{H}_a \mathbf{H}_a^H \right) \end{bmatrix}, \end{aligned} \tag{9}$$

with the scalar constant

$$\begin{aligned} c = h_a^2 h_b^2 - |\mathbf{h}_1^H \mathbf{h}_3|^2 - |\mathbf{h}_2^H \mathbf{h}_3|^2 - |\mathbf{h}_2^H \mathbf{h}_4|^2 - \\ - |\mathbf{h}_1^H \mathbf{h}_4|^2 - \Re\left\{ \mathbf{h}_1^H \mathbf{h}_3 \mathbf{h}_2^H \mathbf{h}_4 - \mathbf{h}_1^H \mathbf{h}_4 \mathbf{h}_2^H \mathbf{h}_3 \right\}, \end{aligned} \tag{10}$$

where $\Re\{.\}$ denotes the real value operator. For the throughput simulations in Section V the ZF/LMMSE receiver was implemented according to (9).

C. ZF-SIC/MMSE-SIC Receiver

The ZF-SIC and MMSE-SIC (ZF and MMSE with Successive Interference Cancelation) receivers are working in the first step exactly like the above mentioned ZF and LMMSE receivers. But after multiplying with the pseudoinverse, the symbol stream with larger signal to noise ratio is detected first and fully decoded and error corrected by the Turbo decoder. The selection criterion which symbol stream is decoded first can be written as

$$\frac{h_a^2}{\mathrm{TBS}_1} \underset{\mathrm{SG2}}{\overset{\mathrm{SG1}}{\gtrless}} \frac{h_b^2}{\mathrm{TBS}_2}, \tag{11}$$

with TBS_k meaning the transport block size (number of information bits in one subframe) of the k-th subgroup. This selection criterion corresponds to the E_b/N_0 of the uncoded bit stream. Note, that this criterion based on the transport block size automatically takes the modulation (QPSK or 16-QAM), as well as the code rate of the channel code into account. After decoding the stronger bit stream in the Turbo decoder, this bit stream is treated like in the transmitter, i.e. interleaved, coded, and mapped to symbols. These reconstructed transmit symbols are then multiplied by the channel matrix and subtracted from the received symbols in order to perform the interference cancelation. After the interference cancelation the remaining subgroup is detected by a standard Alamouti receiver [2].

D. MMSE-pSIC Receiver

The above mentioned receiver with interference cancelation has two major drawbacks:

1) It is expensive to implement, since the whole coding of the transmitter has to be performed before interference cancelation.
2) It has a large decoding delay because the decoding of the second subgroup can not start before the first subgroup is decoded and encoded again.

Therefore, the question arises if it is really necessary to perform the whole decoding operation before doing interference cancelation. In particular, we investigated a receiver which performs the interference cancelation with hard decision values of the symbols obtained by the linear MMSE receiver. We call this receiver the MMSE-pSIC (MMSE with partial Successive Interference Cancelation).

E. ML Receiver

The ML (Maximum Likelihood) receiver decides

$$\hat{\mathbf{z}} = \arg\min_{\mathbf{z}} \|\mathbf{G}\mathbf{z} - \mathbf{r}\|_2^2. \tag{12}$$

Unfortunately, this minimization problem yields only hard decision values of the transmit symbol vector, which results in combination with the Turbo decoder in very poor performance. Therefore, a MAP receiver that a posteriori estimates the log-likelihood ratio (LLR) of every codeword bit, is desireable. The LLR value for the k-th bit can be calculated from

$$\mathrm{LLR}(b_k) = \log \frac{\sum_{\mathbf{z}|b_k=1} \exp\left(-\frac{1}{2} \frac{\|\mathbf{G}\mathbf{z}-\mathbf{r}\|_2^2}{\sigma_v^2} \right)}{\sum_{\mathbf{z}|b_k=0} \exp\left(-\frac{1}{2} \frac{\|\mathbf{G}\mathbf{z}-\mathbf{r}\|_2^2}{\sigma_v^2} \right)}, \tag{13}$$

where the summation in the nominator is over all transmit symbol vectors with bit $b_k = 1$ and the summation in the denominator is over all symbol vectors with bit $b_k = 0$. Since this direct calculation of the LLR values has rather high complexity, the ML receiver was only implemented for QPSK transmission. The high complexity of the direct LLR calculation can be greatly reduced by using a max-log-map approximation. We did not follow this approach, since the results shown in the next section reveal that the ML performance of the exact implementation is not significantly better than the performance of the MMSE-SIC or the MMSE-pSIC.

TABLE I

COMMON SIMULATION PARAMETERS.

Parameter	Value
UE capability class	6
Max. no. of retransmissions	3
Combining	soft
RV coding sequence	$\{0, 2, 5, 6\}$
P − CPICH E_c/I_{or}	−10 dB
SCH E_c/I_{or}	−12 dB
P − CCPCH E_c/I_{or}	−12 dB
OCNS	on
$\hat{I}_{or}/I_{oc}$	10 dB
Channel coefficient estimation	least squares
Turbo decoding	max-log-MAP - 8 iterations

TABLE II

SISO AND STTD SIMULATION PARAMETERS.

Parameter	Value
Modulation	QPSK
Transport block size	720
Coding rate	3/4
No. of channelization codes	5
Peak data rate	1.8 Mbps

V. THROUGHPUT RESULTS

An overview of the simulation parameters used is given in Tables I, II, and III. Table I shows the common simulation parameters of the HSDPA simulator. Reference [7] explains these parameters in detail.

We used fixed channel quality indicator (CQI) values for all simulations. Every CQI corresponds to a specific coding rate and modulation. Since the CQI values have different meaning for DSTTD and SISO transmission, we used the CQI values proposed for DSTTD [5] in our simulations and tried to find comparable settings for the SISO and STTD transmissions. Note, that in contrast to SISO HSDPA the CQI value for DSTTD does not specify the number of channelization codes assigned to the user. Therefore, we used a fixed number of spreading codes for our simulations.

All simulations were performed for several HS-PDSCH E_c/I_{or} (chip energy of the data stream over total radiated energy) values. The $\hat{I}_{or}/I_{oc}$ ratio is defined at the UE and is the ratio between the mean energy received from the desired Node B and the mean interferer energy. We assumed

TABLE III

DSTTD SIMULATION PARAMETERS.

Parameter	Value	
CQI	6	
Modulation	QPSK	
Subgroup	SG1	SG2
Transport block size	720	720
Coding rate	3/4	3/4
No. of channelization codes	5 (3)	
Peak data rate	3.6 Mbps (2.16 Mbps)	

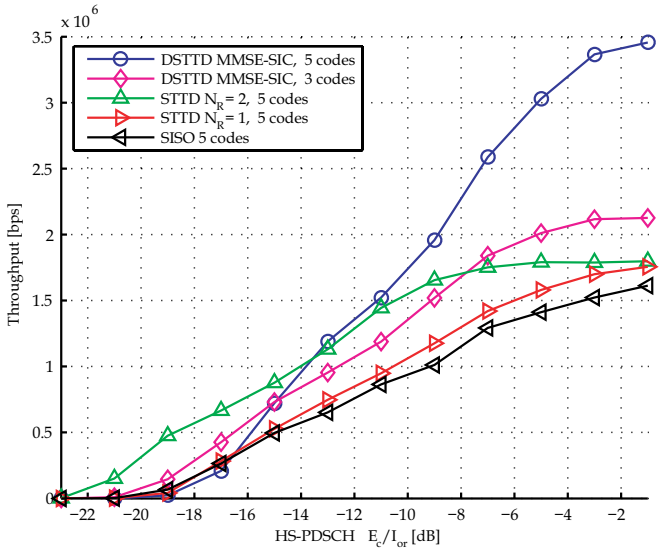

Fig. 1. Throughput comparison between DSTTD, STTD, and SISO.

an $\hat{I}_{or}/I_{oc} = 10$ dB and modeled the interferers evolving from other basestations as additive white Gaussian noise. This assumption is feasible since the different basestations are using different scrambling sequences.

A. DSTTD, STTD, and SISO Throughput Comparison

One objective of the throughput simulations was to evaluate the performance of DSTTD ($N_R = 2$) in comparison to the SISO and the optional, but already standardized, STTD transmission scheme. Fig. 1 shows this comparison for the MMSE-SIC receiver and QPSK transmission. It can be seen that for high E_c/I_{or} (The typical operating point would be slightly before achieving the peak data rate of the specific CQI level.), DSTTD with the same number of spreading codes achieves slightly more than twice the performance of the SISO transmission. It can also be seen that for low E_c/I_{or} the STTD transmission with two receive antennas outperforms DSTTD. However, in DSTTD mode the UE would report a worse CQI level to the Node B at low E_c/I_{or} resulting in a lower coding rate for the next transmitted subframe. Note, that this lower coding rate leads to a higher throughput since fewer retransmissions are necessary.

When comparing STTD with one receive antenna to SISO we notice that STTD performs about 2-3 dB better in E_c/I_{or}, but only about 10-15% in throughput.

B. DSTTD Throughput for Different Receivers

The next simulation was accomplished to investigate the impact of the various receiver structures on the system throughput. This comparison is shown for a QPSK transmission in Fig. 2. The MMSE-SIC receiver achieves the ML throughput at low E_c/I_{or} and about 94% of the ML throughput at high E_c/I_{or}. At the cost of an additional throughput loss of about 3-4% a significant reduction in receiver complexity is possible by using the before introduced MMSE-pSIC receiver. Therefore,

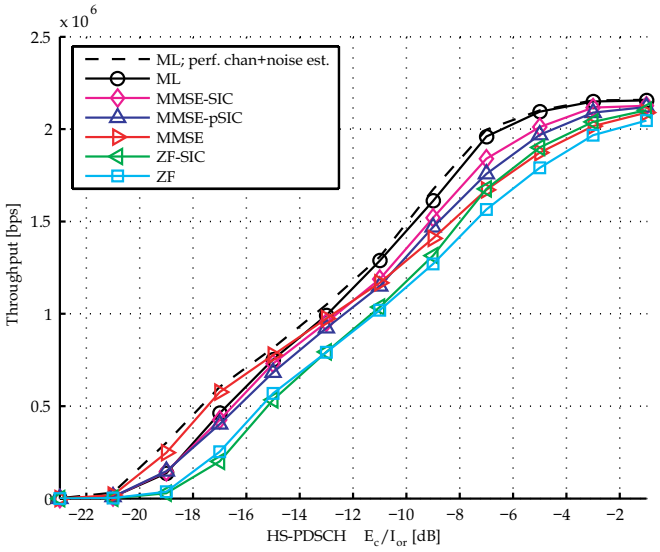

Fig. 2. Different receivers for DSTTD QPSK transmission and 3 channelization codes, $N_R = 2$.

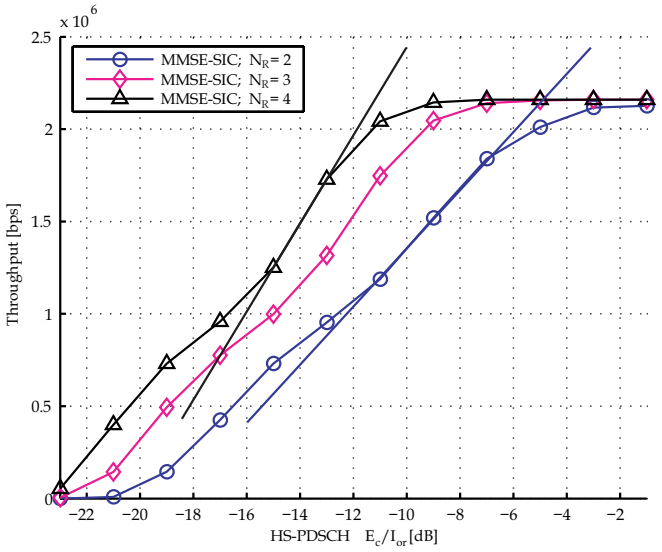

Fig. 3. Different number of receive antennas, 3 channelization codes.

the MMSE-pSIC receiver is a low complexity receiver for user equipments achieving about 90% of the ML performance.

C. DSTTD Throughput for Multiple Receive Antennas

The impact of a third and fourth receive antenna at the user equipment is illustrated in Fig. 3. These additional receive antennas achieve higher receive diversity making the system more robust against fading. The steeper slopes of the throughput curves indicate this higher diversity. Furthermore, the array gain of the receive antennas result in higher receive SNR, shifting the throughput curves to the left.

It can also be seen in Fig. 3 that the throughput achieves the peak data rate of the specific CQI level at rather low E_c/I_{or} values. Thus, the user equipment would report a better CQI value to the Node B leading to even higher throughput than shown in the plot.

VI. Conclusions

We have shown throughput simulations for DSTTD-SGRC, a candidate for the MIMO extension of UMTS HSDPA. A comparison between DSTTD, STTD and SISO shows that DSTTD in a 4×2 system is able to achieve slightly more than twice the throughput of a corresponding SISO transmission. Additionally, we derived an LMMSE receiver that does not require a matrix inversion and can be used as a first stage of the MMSE-pSIC receiver. This MMSE-pSIC receiver achieves about 90 % of the ML performance, thus, allowing low complexity receivers in the UE with very good performance. However, as shown by [11] it is known that the DSTTD code is sensitive to high spatial channel correlation. Therefore, further investigations of the DSTTD-SGRC proposal have to include more sophisticated MIMO channel models to show the impact of spatial correlation on the system throughput. Furthermore, simulations and comparisons of the other MIMO HSDPA proposals have to be carried out to find the best proposal in terms of throughput and complexity.

Acknowledgments

This work has been funded by the Christian Doppler Laboratory for Design Methodology of Signal Processing Algorithms as well as **K***plus*, Infineon Technologies and the ARC Seibersdorf Research GmbH (ARCS) through ftw. Projects C3 and C9.

References

[1] 3GPP, "Technical specification group radio access network; physical channels and mapping of transport channels onto physical channels (FDD)," 3GPP, Tech. Rep. 25.211 V6.3.0, Dec 2004.

[2] S. M. Alamouti, "A simple transmit diversity technique for wireless communications," *IEEE Journal on Selected Areas in Communications*, vol. 16, no. 8, pp. 1451–1458, Oct 1998.

[3] G. J. Foschini and M. J. Gans, "On limits of wireless communication in a fading environment when using multiple antennas," *Wireless Personal Communications*, vol. 6, no. 3, pp. 311–335, 1998.

[4] I. E. Telatar, "Capacity of multi-antenna gaussian channels," *European Transactions on Telecommunications, 1999, Technical Memorandum, Bell Laboratories, Lucent Technologies*, vol. 10, no. 6, pp. 585–595, Oct 1998.

[5] 3GPP, "Technical specification group radio access network; Multiple-Input Multiple Output in UTRA," 3GPP, Tech. Rep. 25.876 V1.7.0, Aug 2004.

[6] ——, "Technical specification group radio access network; user equipment (UE) radio transmission and reception (FDD)," 3GPP, Tech. Rep. 25.101 V5.11.0, Jun 2004.

[7] F. Kaltenberger, K. Freudenthaler, S. Paul, J. Wehinger, C. F. Mecklenbräuker, and A. Springer, "Throughput enhancement by cancelation of synchronization and pilot channel for UMTS high speed downlink packet access," in *Proc. SPAWC 2005*, New York, USA, Jun 2005.

[8] 3GPP, "Technical specification group radio access network; multiplexing and channel coding (FDD)," 3GPP, Tech. Rep. 25.212 V5.9.0, Jun 2004.

[9] C. Mecklenbräuker and S. Paul, "A novel pilot pattern definition for the downlink of UMTS with 4 Tx antennas," in *Proc. IEEE Workshop on Smart Antennas WSA 2005*, Duisburg, Germany, Apr 2005.

[10] M. Harteneck, M. Boloorian, S. Georgoulis, and R. Tanner, "Practical aspects of an HSDPA 14 Mbps terminal," in *Conference Record of the Thirty-Eighth Asilomar Conference on Signals, Systems and Computers, 2004*, Pacific Grove, CA, USA, Nov 2004.

[11] G. Gritsch, G. Kolar, H. Weinrichter, and M. Rupp, "Two adaptive space-time block coded MIMO systems exploiting partial channel knowledge at the transmitter," in *Proc. 5th International ITG Conference on Source and Channel Coding (SCC)*, Erlangen, Germany, Jan 2004.